Supporting Information

In Situ Annealing Effect on Thermally Co-Evaporated $CsPbI_2Br$ Thin Films Studied via Spectroscopic Ellipsometry

Athina Papadopoulou[1,2]*, Rafikul Ali Saha[3], Maria Isabel Pintor-Monroy[1], Wenya Song[1], Itai Lieberman[1], Eduardo Solano[4], Maarten B. J. Roeffaers[3], Robert Gehlhaar[1], and Jan Genoe[1,2]*

[1]imec, Kapeldreef 75, 3001 Leuven, Belgium
[2]Department of Electrical Engineering (ESAT), KU Leuven, Kasteelpark Arenberg 10, 3001 Leuven, Belgium
[3]cMAS, Department of Microbial and Molecular Systems, KU Leuven, Celestijnenlaan 200F, 3001 Leuven, Belgium
[4]NCD-SWEET Beamline, ALBA Synchrotron Light Source, Cerdanyola del Vallès, Barcelona 08290, Spain

*Email: athina.papadopoulou@imec.be, jan.genoe@imec.be

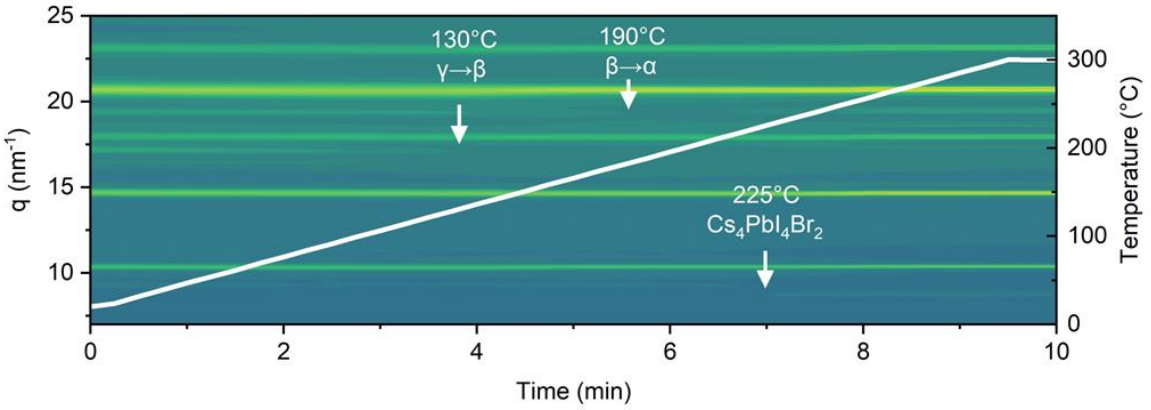

Figure S1. In situ reduced 1D GIWAXS data during the temperature ramp. Phase transitions and the associated temperatures are also indicated. In order to investigate the origin of the peak that appears at 8.7 nm^{-1} at 225°C we consider the 1D integrated GIWXAS signal at the end of the annealing ramp (shown in **Figure 1b**). It has been previously shown that the 0D phase of Cs_4PbX_6 can emerging during the annealing of all-inorganic perovskite films. Both Cs_4PbI_6 and Cs_4PbBr_6 are stabilized in the same crystal structure (trigonal space group R-3c), which indicates that iodine (I) and bromine (Br) can substitute for each other without altering the crystal geometry. The only difference between them lies in the lattice parameters (unit cell volume) due to the ionic radius mismatch between I^- (2.2 Å) and Br^- (1.96 Å) for the same coordination geometry. As expected, the larger ionic radius of I^- results in larger lattice parameters for Cs_4PbI_6 (a = b = 14.602 Å, c = 18.268 Å)[1] compared to Cs_4PbBr_6 (a = b = 13.722 Å, c = 17.299 Å)[2]. In our case, the lattice parameters are measured as a = b = 14.138 Å, c = 17.828 Å, clearly indicating that some of the iodine has been replaced by bromine. Further analysis through Rietveld refinement, including occupancy refinement, confirms a stoichiometry of $Cs_4PbI_4Br_2$. During the refinement process, we considered two distinct phases, γ-$CsPbI_2Br$ and $Cs_4PbI_4Br_2$, which successfully accounted for all the peaks in the X-ray diffraction (XRD) pattern. No additional peaks were observed, ruling out the presence of any other impurity phases. The formation of $Cs_4PbI_4Br_2$ complicates the overall stoichiometry of the main phase. One possibility is that the stoichiometric mismatch may exist as an amorphous component within the material, but the amount is minimal and unlikely to affect the main phase's properties significantly.

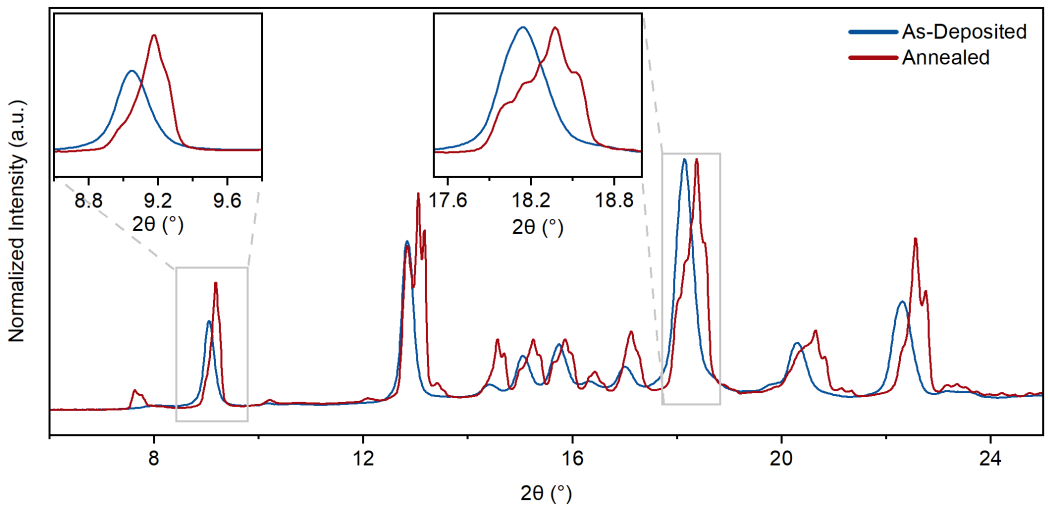

Figure S2. Comparison of GIWAXS 2θ signals for the As-Deposited and Annealed state. The insets provide a close-up of selected peaks. Three key changes can be clearly observed: (i) peak shifting, (ii) a reduction in the full width at half maximum (FWHM) due to annealing, and (iii) the appearance of peak asymmetry or splitting after annealing. The reduction in FWHM is particularly notable, as it highlights the peak asymmetry or splitting more distinctly, indicating that annealing has led to an increase in the average crystallite size. This observation is further supported by crystallite size calculations using Scherrer's equation: $D = \frac{k \times l}{\beta \times cos\,\theta}$; Where k is the shape factor (0.9), l is x-ray wavelength (0.09574 nm), β is the FWHM of the peak, and θ is the Bragg peak position in radians. These calculations indicate that the crystallite size nearly doubled as a result of the annealing process. In addition to the increase in crystallite size, the nonuniform peak shift towards right side and the appearance of peak asymmetry suggest that the annealing process has introduced macrostrain into the system. This strain could be attributed to two main factors: (i) the mismatch in the thermal expansion coefficients between the substrate and the thin film, which can induce biaxial strain at the interface[3], and (ii) the coexistence of the 0D $Cs_4PbI_4Br_2$ phase and the 3D $CsPbI_2Br$ phase, which may create lattice anchoring within the system[4,5].

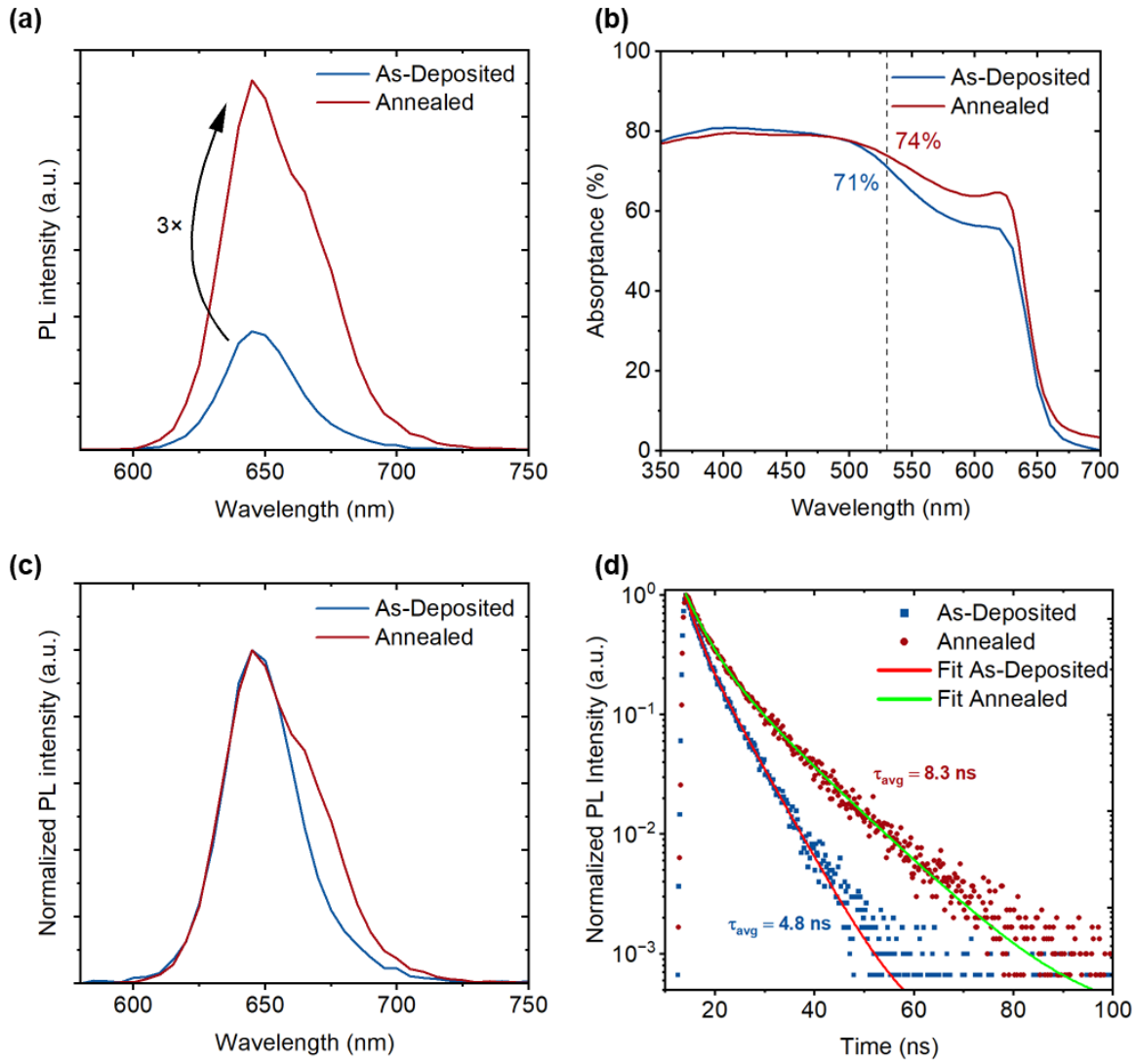

Figure S3. (a) SSPL spectra, (b) Absorptance spectra, (c) Normalized SSPL spectra, and (d) TRPL spectra for the As-Deposited and Annealed sate.

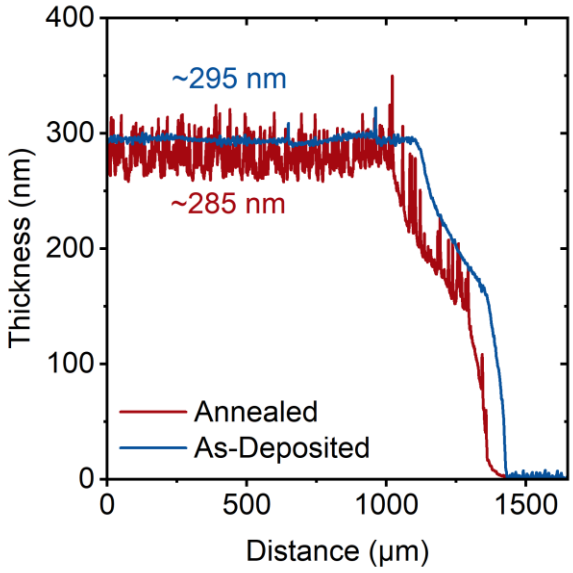

Figure S4. Profilometry results for the As-Deposited and Annealed state.

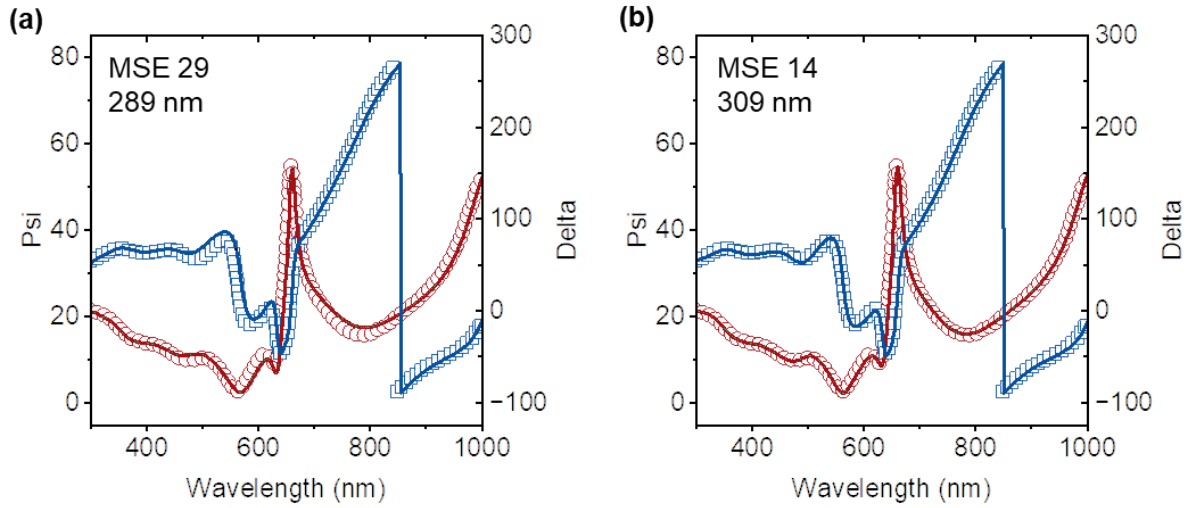

Figure S5. Comparison between the SE experimental (open symbols) and fitted results (solid lines) for the Annealed state (a) with 50% voids in the roughness layer and fixed bulk thickness, and (b) with 50% voids in the roughness layer and fitted bulk thickness. The MSE of each fit, as well as the estimated thickness of the bulk perovskite layer is indicated in each figure. The model that provided (a) was rejected because of high MSE. The model that provided (b) was rejected because the estimated bulk thickness does not match with the profilometry measurements.

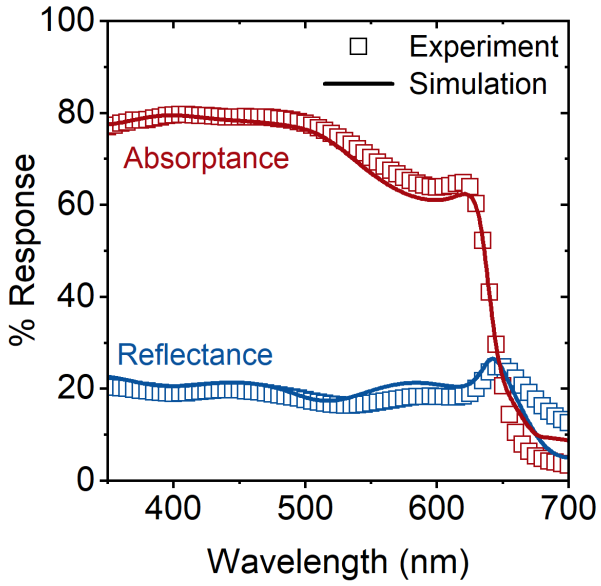

Figure S6. Comparison between the experimental (obtained through R/T measurements) and simulated (obtained with a transfer matrix algorithm and SE-derived nk values) spectra of Reflectance and Absorptance for the Annealed state.

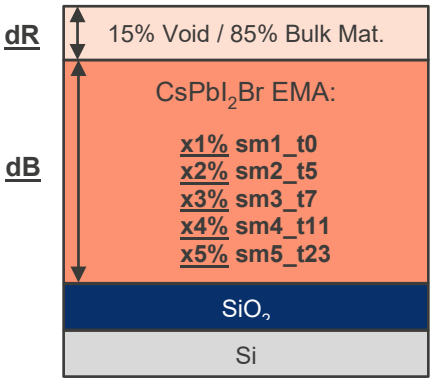

Figure S7. Schematic of the optical model used for the dynamic ellipsometry fitting. The bulk layer consists of the five static models, shown in Figure S8. The parameters of these models are fixed, but the percentage of their volume fraction is fitted. The roughness layer consists of 15% voids.

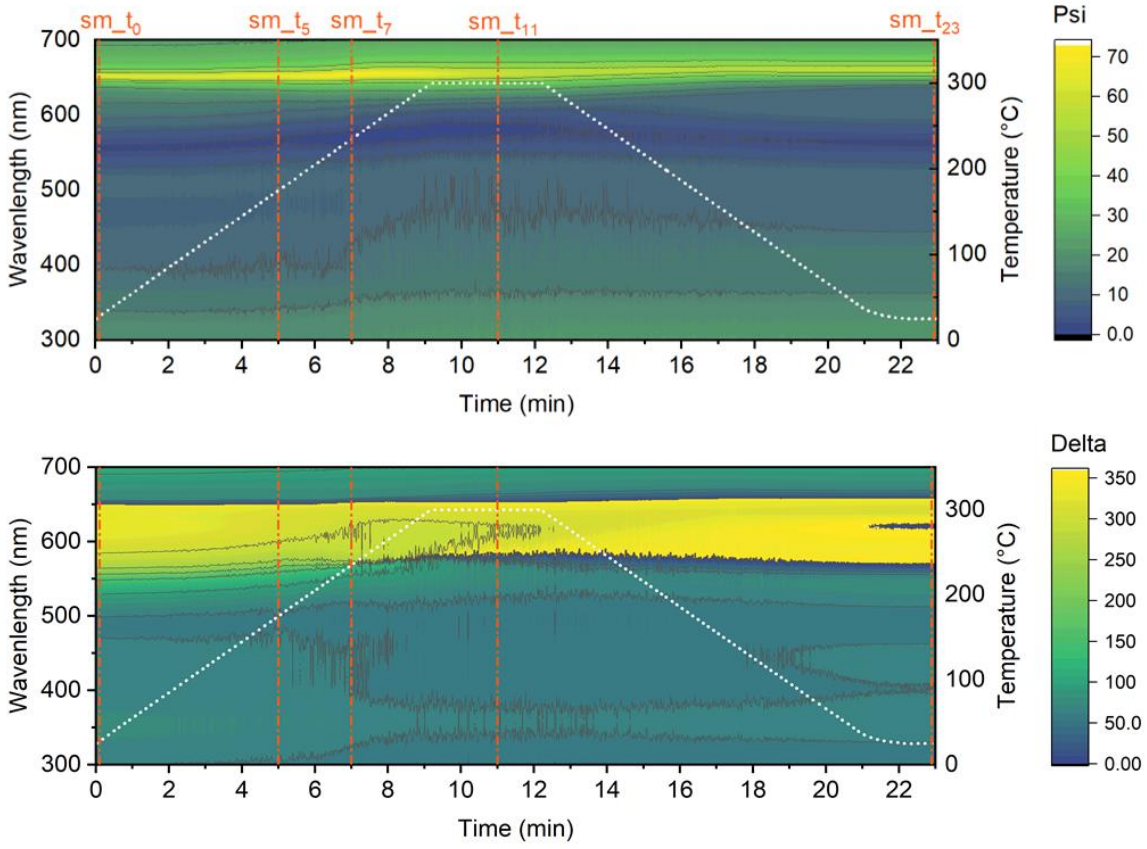

Figure S8. Evolution of raw ellipsometry data as a function of time a temperature for wavelengths. The data range has been limited to 300 – 700 nm for a clearer visual representation. The red dashed lines indicate the timestamps for which a static model was developed.

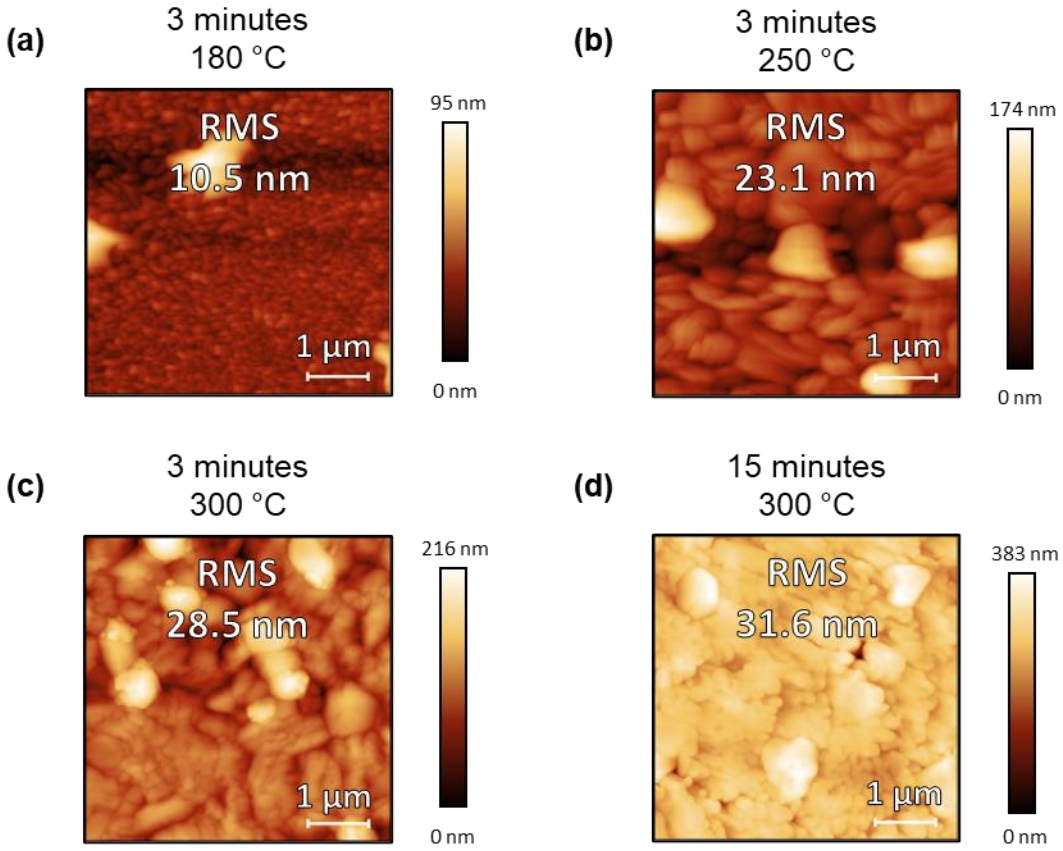

Figure S9. AFM image of a $CsPbI_2Br$ sample annealed (a) for 3 minutes at 180°C and (b) for 3 minutes at 250°C. AFM image of the Annealed state of a $CsPbI_2Br$ sample exposed to (c) the heating ramp of Figure 1a and (d) the same heating ramp with a 15-minute stabilization period at 300°C.

References:

1. Bhaumik, S., Bruno, A. & Mhaisalkar, S. Broadband emission from zero-dimensional Cs4PbI6 perovskite nanocrystals. *RSC Adv* **10**, 13431–13436 (2020).
2. De Bastiani, M. *et al.* Inside Perovskites: Quantum Luminescence from Bulk Cs4PbBr6 Single Crystals. *Chemistry of Materials* **29**, 7108–7113 (2017).
3. Steele, J. A. *et al.* Thermal unequilibrium of strained black $CsPbI_3$ thin films. *Science (1979)* **365**, 679–684 (2019).
4. Steele, J. A. *et al.* An embedded interfacial network stabilizes inorganic $CsPbI_3$ perovskite thin films. *Nature Communications 2022 13:1* **13**, 1–11 (2022).
5. Saha, R. A. *et al.* Oxygen-Mediated (0D) Cs4PbX6 Formation during Open-Air Thermal Processing Improves Inorganic Perovskite Solar Cell Performance. *ACS Nano* **18**, 16994–17006 (2024).